SciMedCentral

JSM Sexual Medicine

Research Article

The Expression of Macropinocytosis-Related Genes in Ovarian Cancer and Their Relationships with Prognosis

Ying Shao[1]*, Shuai Huang[2], and Zhaochun He[3#]

[1]*Department of Surgical Pathology, Zhejiang University, China*

[2]*Department of Surgical Pathology, Zhejiang University, China*

[3]*Department of Rheumatoid Immunity, the Second Affiliated Hospital of Zhejiang Chinese Medical University, China*

[#]*both the authors contributed equally*

***Corresponding author**

Ying Shao, Department of Surgical Pathology, Women's Hospital, School of Medicine, Zhejiang University, Hangzhou, Zhejiang Province, China

Submitted: 08 November 2023

Accepted: 30 November 2023

Published: 30 November 2023

ISSN: 2578-3718

Keywords

- Ovarian cancer
- EZR
- HSPG2
- SLC9A1
- Macropinocytosis

Abstract

Background: The mechanism of macropinocytosis has been reported in receptor sorting used by motile cells. Besides, the role of macropinocytosis was previously recognized in cancer progression. We evaluated the prognostic value of macropinocytosis gene expression in ovarian cancer (OC).

Method: Ten candidate genes were selected in the intersection between 134 macropinocytosis-related genes from Gene cards database and 2925 OC prognostic genes using the Cancer Genome Atlas (TCGA) database. Heat map showed ten candidate genes expression. Gene ontology (GO) and Kyoto encyclopedia of genes and genomes (KEGG) analysis was conducted on the ten candidate genes. Protein–protein interactions were constructed using the STRING database. Hub genes were identified based on PPI networks. The key hub genes were selected both in differential expression analysis and Kaplan-Meier survival analysis. Then we identified transcription factor-gene interaction. The relationships between clinical characteristics and the key hub genes expression were performed with T test. Clinicopathologic factors correlated with overall survival (OS) conducting univariate, multivariate and LASSO Cox regression analyses. Human Protein Atlas (HPA) databases were utilized to verify the results. Furthermore, Gene Set Enrichment Analysis (GSEA) identified the potential key pathways that dominate macropinocytosis in OC.

Result: Elevated EZR, HSPG2 and SLC9A1 expression was significantly associated with OC poor survival and clinical features. Transcription factor-gene interaction and GSEA analysis reported many key regulators and signaling pathways that were enriched in OC with varying degrees of macropinocytosis-related genes expression.

Conclusions: The three macropinocytosis-related genes might be utilized as new candidate prognostic biomarkers for OC.

INTRODUCTION

Ovarian cancer (OC) is the most lethal gynaecological malignancies and possesses a high capacity for metastasis [1]. OC metastasizes either by direct extension from the ovarian/fallopian tumor to neighboring organs (bladder/colon) or when cancer cells detach from the primary tumor [2]. An in-depth understanding of the cellular and molecular mechanisms of OC metastasis are crucial for developing effective preventative measures.

Macropinocytosis is a unique pinocytosis process by which cancer cells internalize extracellular proteins or necrotic cell debris and deliver them to lysosomes for further degradation. During tumor development, macropinocytosis provide not only a survival possibility under nutritional deficiencies for cancer cells, but also the potential for tumors to limitlessly grow in harsh tumor microenvironments [3]. Macropinocytosis is drived by actin cytoskeleton remodeling. Several actin polymerization regulators, such as small GTPases, p21-activated kinase 1 (Pak1), and PI3K, have been related to the formation of plasma membrane protrusions and macropinocytic activity [4]. Recently, one study showed that the internalization of eATP by macropinocytosis in human lung cancer cells could drive epithelial-mesenchymal transition (EMT) to induce metastasis [5]. Another study also reported that cadherin-6B was removed from premigratory neural crest cells through internalization induced by macropinocytosis, then promoted EMT and migration [6]. These studies revealed the significance of macropinocytosis in the tumor metastasis. Up to now, some studies showed that macropinocytosis had the advantage for the drug delivery in OC

therapy [7,8]. However, a clear potential of macropinocytosis-related genes with prognostic meaning and clinical diagnosis in OC has not yet been more comprehensively studied.

Accordingly, the establishment of new biomarkers related to macropinocytosis is crucial for the early detection and prognosis of OC. The Cancer Genome Atlas (TCGA) database was used to analyze the clinical information of OC and mRNA expression difference in normal and OC tissues. The key hub genes were selected from 134 candidate macropinocytosis-related genes for subsequent correlation analyses of clinical factors, univariate, multivariate and LASSO Cox regression analyses. To identify the contribution of the key hub genes to the signaling pathway related to macropinocysis, Gene Set Enrichment Analysis (GSEA) was worked for functional enrichment analysis. Furthermore, Human Protein Atlas (HPA) was applied to render verification support to our outcomes from TCGA. This study was conducive to the enormous potential of macropinocysis-related genes as a new prognostic marker of OC in the future.

MATERIALS AND METHODS

Data extraction and arrangement

The workflow of this study is shown in Figure 1. To explore the key genes and pathways which affect OC metastasis, macropinocytosis-related genes were selected from the Gene Cards database (protein coding and relevance score > 1). The whole transcriptase sequencing data set of raw read counts and fragments per kilo base per million (FPKM) data and corresponding clinical data of all ovarian OC patients were downloaded from the TCGA database (n=381) for collecting overall survival data, and then ranked according to P-value (P<0.05). To obtain macropinocytosis genes related to OC prognosis, we intersected macropinocytosis-related genes and OC prognostic genes. The candidate genes were found in the intersection. Then we combined TCGA with normal tissues from the Genotype-Tissue Expression (GTEx) data from Xena database (tumor tissues = 427, normal tissues= 88) for further analyses. The candidate genes expression heat map was produced using the ComplexHeatmap R package (2.13.1).

Gene ontology (GO) and Kyoto encyclopedia of genes and genomes (KEGG) pathway enrichment analyses

To comprehensively investigate the biological meaning behind the candidate genes, cluster Profiler 4.4.4 was used to obtain the set of functional annotation. GO is an extensively used tool for annotating genes with potential functions, such as molecular function (MF), biological pathways (BP) and cellular components (CC). KEGG enrichment analysis is a practical resource for analytical study of gene functions and associated high-level genome functional information. P<0.05 was regarded as the threshold value. Results were visualized with ggplot2 3.3.6.

Protein-protein Interactions (PPIs) network and hub gene analysis of the candidate genes

All candidate genes were subject to PPI network analysis utilizing STRING database with the median confidence 0.4 [9]. Cytoscape (v3.10.0) was used to visualize the PPI network. Both the color and the size of the nodes indicates the score calculated using degree topological analysis methods.

Extraction of hub genes

Cytoscape software was applied to analyse the hub genes, which are important nodes with many interaction partners. We utilized the cytoHubba plugin in Cytoscape to identify the hub genes [10]. Determination of the top 20 genes depends on the

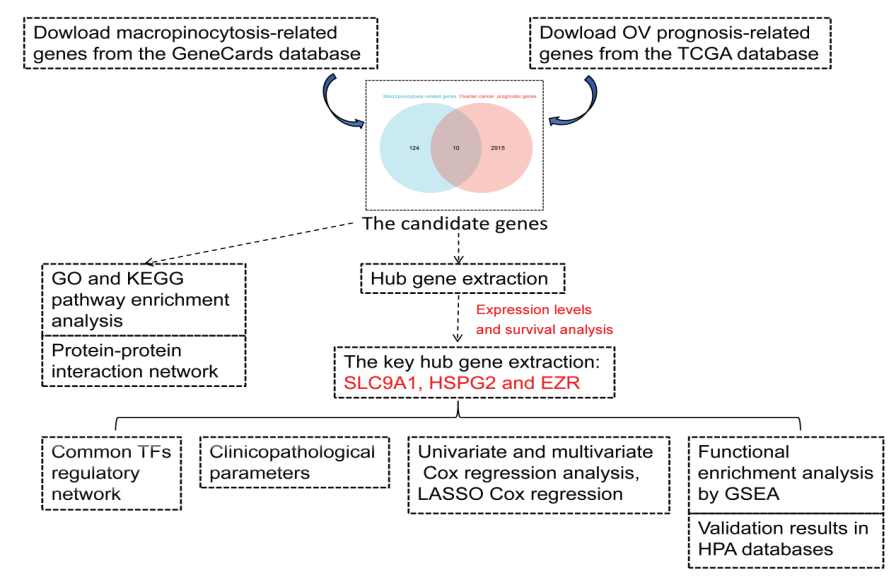

Figure 1 The flowchart of our research process

BottleNeck algorithm. The ranks of hub genes are represented by a gradient from red to yellow. Finally, the hub genes were ranked for the shortest accessible paths between hub genes, making them easier to observe.

Expression level and survival analyses of the Hub genes in OC

The gene expression level and OC patients survival was analyzed in R (4.2.1), and data was visualized using ggplot2 [3.3.6]. Briefly, RNA sequencing expression and survival data from TCGA and GTEx project was used to perform the key hub genes expression differences analyses in normal and OC tissues by Wilcoxon rank sum test. Only the samples with both survival status and survival time information could be used for overall survival (OS), progress free interval (PFI) and disease specific survival (DSS). Kaplan-Meier survival curves were evaluated using the long-rank test. Only genes with high expression level and low survival time in tumor tissues (P-value < 0.05) could be considered as the key hub genes with significant differences for subsequent analyses.

Identification of transcription factors associated with the key hub genes

Transcription factors (TFs) control chromatin and transcription by identifying specific DNA sequences [11]. In addition to controlling genome expression, they provide essential information for molecular understanding. We explored the regulatory effects of the TFs on the key hub genes through the TFs retrieved from the Chip Base database [12], and then obtained a set of common TFs by taking the intersection of these TFs. Finally, the Cytoscape software was used to visualize the common TFs of the key hub genes.

Correlation analysis of clinical factors and univariate, multivariate and LASSO Cox regression analyses from TCGA database

The clinical data that removed missing information was conducted to visualize the key hub genes expression differences in clinical characteristics respectively. T test was used between two groups. Univariate and multivariate Cox regression analyses were implemented to identify independent prognosis risk factors. Only factors with entire information in age, clinical stage, histologic grade, venous invasion, lymphatic invasion, and gene expression were assessed for prognosis risk factors. All comparisons were considered statistically significant with a P-value < 0.05. Forest map was used to visualize the univariate Cox regression analyses with the ggplot2 3.3.6. We next used LASSO Cox regression to visualize the risk score and grouping of the prognostic model with ggplot2 3.3.6.

Identification of relevant signaling pathways of the key hub genes by Gene Set Enrichment Analysis (GSEA)

GSEA was performed using the R package cluster Profiler [4.4.4] for functional enrichment analysis from the TCGA database to investigate possible biological functions of the key hub genes, including GO Enrichment, DO Enrichment, KEGG Enrichment and Reactome Enrichment. The following parameters were set to run the enrichment test. The name of each gene was selected as the expression dataset, and "c2.cp.all.v2022.1.Hs.symbols.gmt" was chosen as the gene sets database. The max size excluded larger sets and the min size excluded smaller sets were set in default values of 500 and 15, respectively. Signaling pathways with a false discovery rate (FDR) q-value < 0.25 was used to select the enriched signaling pathways when adjusted P-value < 0.05.

The tissue-level of the key hub genes expression in Human protein atlas

The location of the key hub genes in the body was further determined by searching for its expression in the HPA (https://www.proteinatlas.org/search/HAMP).

RESULT

Data extraction and arrangement

134 genes that relate to macropinocytosis were selected from the Gene Cards database. The intersection between macropinocytosis-related genes and OC prognostic genes (2925 genes, P < 0.05) from TCGA were regarded as candidate genes. In total, we identified 10 candidate genes as follows: ARHGEF26, SNX33, PAK1, SLC9A1, LRP1, HSPG2, UBAP2, CXCR4, SLC38A5 and IL32 Figure 2A. Then we combined TCGA with normal tissues from GTEx database to construct a gene expression heat map to visualize the expression levels of the 10 candidate genes Figure 2B.

GO and KEGG pathway enrichment analysis

Function annotation analysis of the 10 candidate genes was performed. We present the top three items for each category in a bar chart and a bubble chart. In GO enrichment analysis, the 10 candidate genes are significantly enriched in the regulation of blood–brain barrier, vascular transport and regulation of actin cytoskeleton organization in BP subsets. Cell–substrate junction, focal adhesion and cell leading edge are in CC subsets. Lipoprotein particle receptor binding, amyloid–beta binding and aromatic amino acid trans membrane transporter activity are in MF subsets. To explore the biological functions and enriched pathways of the 10 candidate genes, KEGG enrichment analysis was performed. The top three pathways identified by KEGG pathway analysis are as follows: salmonella infection, regulation of actin cytoskeleton and proteoglycans in cancer Figure 2C and 2D.

Identification of the Hub Genes and selection of the key hub genes

The ten candidate genes were uploaded to STRING to explore the network of PPI. PPI network map was visualized through Cytoscape software to identify common gene interaction Figure 2E.

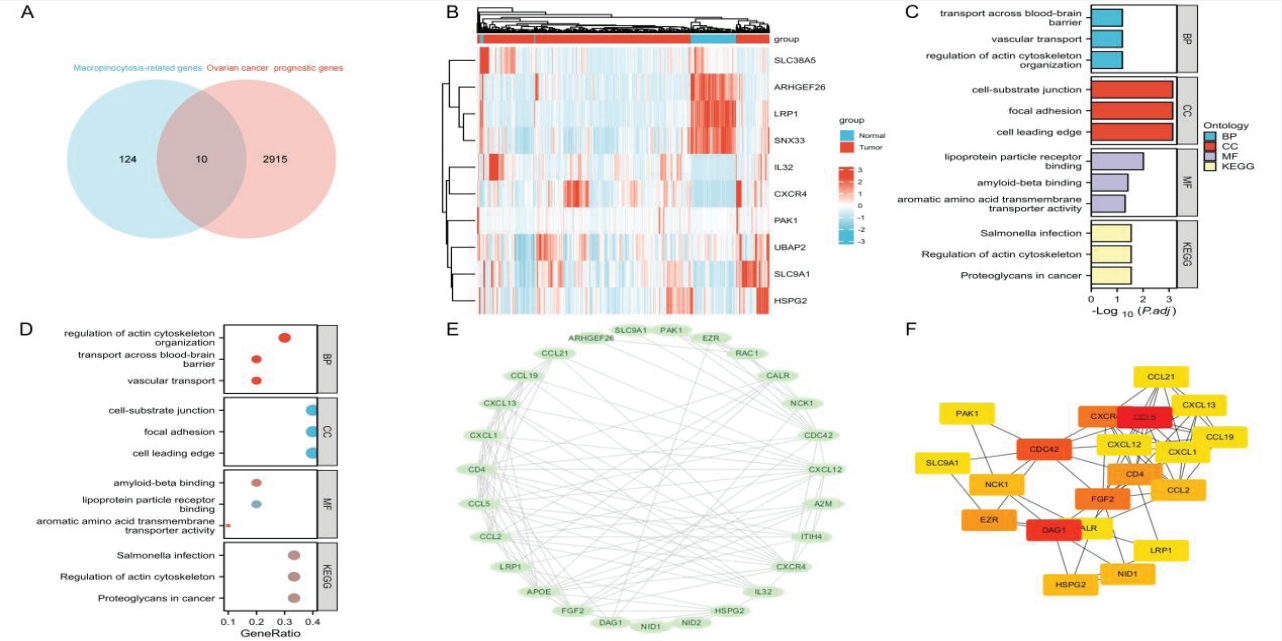

Figure 2 The data extration, expression levels and function annotation analysis of the macropinocytosis-related candidate genes in OC. Identification of the Hub Genes and selection of the key hub genes. (A). The intersection between macropinocytosis-related genes and OC prognostic genes from the TCGA was regarded as the candidate genes; (B). The heat map of the ten screened macropinocytosis-related candidate genes in normal (88 tissues) and OC tissues (427 OC samples) from the TCGA and GTEx database; (C-D) GO and KEGG pathway enrichment of the ten candidate genes; (E) The PPI network was used to identify common gene interaction shared between the ten candidate genes. Cytoscape was used to visualize the PPI network; (F) The identification of the most significant hub genes through BottleNeck method using the CytoHubba plug-in in Cytoscape, including CCL5, DAG1, CDC42, CXCR4, FGF2, EZR, CD4, NCK1, NID1, HSPG2, CCL2, CXCL1, CCL19, CXCL12, SLC9A1, CCL21, CXCL13, PAK1, CALR and LRP1. OC, ovarian cancer; TCGA, the Cancer Genome Atlas; GO, Gene ontology; KEGG, Kyoto encyclopedia of genes and genomes; BP, biological process; CC, cellular components; MF, molecular function; CCL5, C-C Motif Chemokine Ligand 5; DAG1, Dystroglycan 1; CDC42, Cell Division Cycle 42; CXCR4, C-X-C Motif Chemokine Receptor 4; FGF2, Fibroblast Growth Factor 2; EZR, Ezrin; CD4, CD4 Molecule; NCK1, NCK Adaptor Protein 1; NID1, Nidogen 1; HSPG2, Heparan Sulfate Proteoglycan 2; CCL2, C-C Motif Chemokine Ligand 2; CXCL1, C-X-C Motif Chemokine Ligand 1; CCL19, C-C Motif Chemokine Ligand 19; CXCL12, C-X-C Motif Chemokine Ligand 12; SLC9A1, Solute Carrier Family 9 Member A1; CCL21, C-C Motif Chemokine Ligand 21; CXCL13, C-X-C Motif Chemokine Ligand 13; PAK1, P21 (RAC1) Activated Kinase 1; CALR, Calreticulin; LRP1, LDL Receptor Related Protein 1.

Subsequently, we identified the most significant hub genes through BottleNeck method using the CytoHubba plug-in in Cytoscape, including CCL5, DAG1, CDC42, CXCR4, FGF2, EZR, CD4, NCK1, NID1, HSPG2, CCL2, CXCL1, CCL19, CXCL12, SLC9A1, CCL21, CXCL13, PAK1, CALR and LRP1 Figure 2F. Then we performed differential expression analyses and survival analyses to select the key hub genes with high expression in tumor tissues and low survival from the twenty hub genes to perform further analyses. We finally analyzed three key hub genes including EZR, HSPG2 and SLC9A1 Figure 3.

The gene expression, survival analysis of the key hub genes and the relations to clinicopathological parameters from TCGA

The gene expressions of EZR (P<0.05, [Figure 3A]), HSPG2 (P<0.05, [Figure 3E]) and SLC9A1 (P<0.05, [Figure 3I]) in OC tumor tissues were higher than those in normal tissues, and the differences were all statistically significant (P<0.05, [Figure 3]). Kaplan-Meier survival analysis showed that high expression of EZR (OS, P=0.028, [Figure 3B]) (DSS, P=0.016, [Figure 3D]), HSPG2 (OS, P=0.018, [Figure 3F]) (DSS, P=0.013, [Figure 3H]) and SLC9A1 (OS, P=0.009, [Figure 3J]) (DSS, P=0.014, [Figure 3L]) all possessed worse prognosis with a poor OS and a poor DSS. Only EZR overexpression possessed a poor PFI (P=0.006, [Figure 3C]). SLC9A1 expression was notably associated with histologic grade (P<0.05, [Figure 4M]). EZR and SLC9A1 expression was significantly related to age (P<0.05, [Figure 4A and 4K]).

Establishment of TF regulatory networks

In order to elucidate the key molecules that bridge OC and macropinocytosis, we conducted a framework to indicate gene regulatory networks involving TFs from the key hub genes. By analyzing the interaction network of TFs, we found 128 potential common TFs that regulate the three key hub genes Figure 5. Our results indicated the potential connections between the key hub genes with common TFs.

Hazard factors affecting patient's survival

The univariate Cox regression analysis uncovered that the

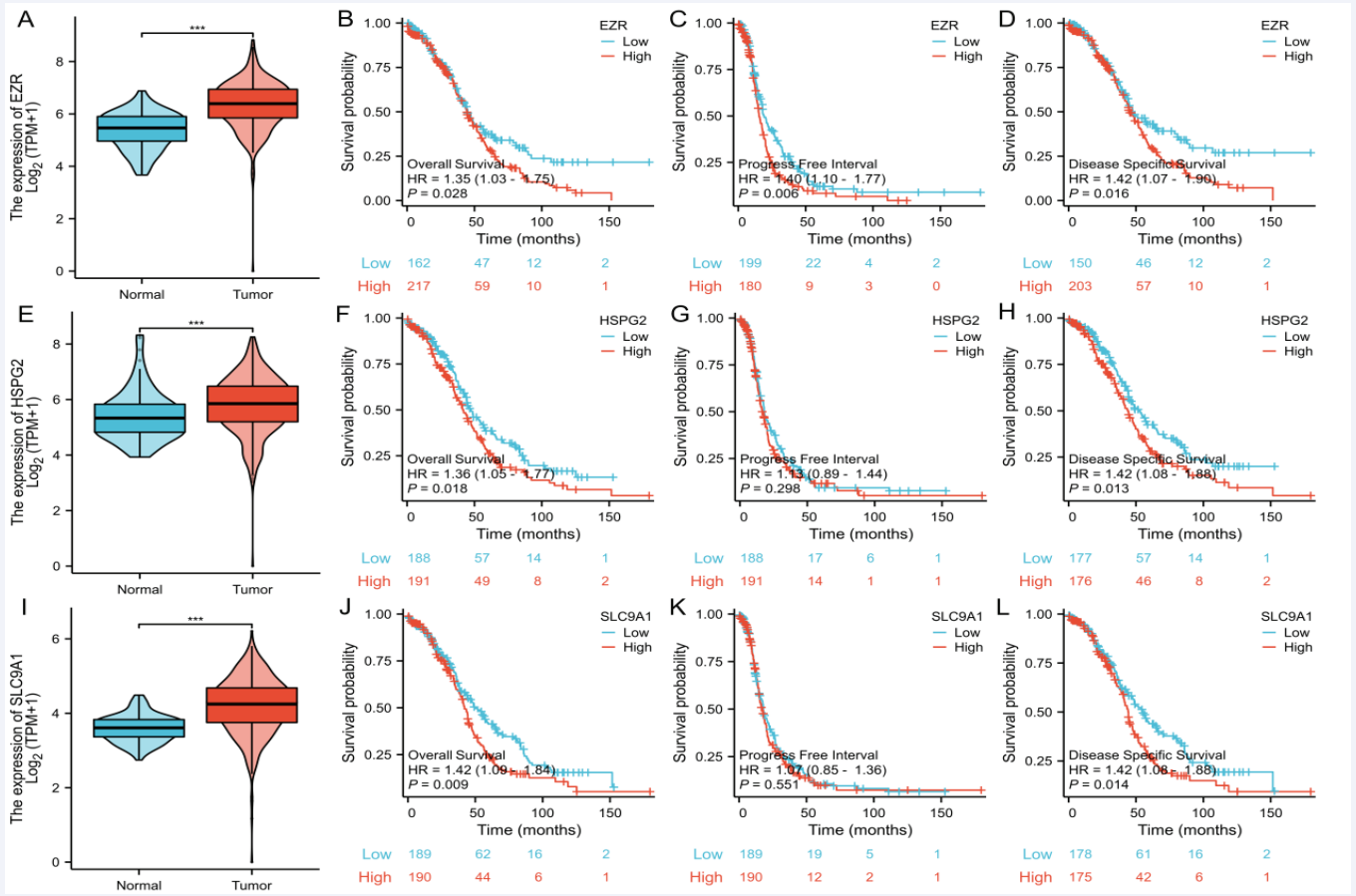

Figure 3 The boxplots and Kaplan-Meier survival curves with mRNA expression of the key hub genes in OC from TCGA database. Different expression of the key hub genes between OC tumor and normal tissues, including EZR (A), HSPG2 (E) and SLC9A1 (F). The higher expression of EZR (OS, P=0.028, Figure 3B) (DSS, P=0.016, Figure 3D), HSPG2 (OS, P=0.018, Figure 3F) (DSS, P=0.013, Figure 3H) and SLC9A1 (OS, P=0.009, Figure 3J) (DSS, P=0.014, Figure 3L) all possessed worse prognosis with a poor OS and a poor DSS. Only EZR overexpression possessed a poor PFI (P=0.006, Figure 3C). OC, ovarian cancer; OS, overall survival rate; PFI, progress free interval; DSS, disease specific survival; EZR, Ezrin; HSPG2, Heparan Sulfate Proteoglycan 2; SLC9A2, Solute Carrier Family 9 Member A1. TCGA, the Cancer Genome Atlas;

up-regulation of EZR, SLC9A1 and HSPG2 expression was related to poor OS in OC Table 1 and Figure 6A. The other clinical variable associated with bad survival was age (hazard ratio [HR]: 1.352; 95% confidence interval [CI]: 1.045–1.749; P = 0.022) Figure 6A and Table 1. In multivariate Cox analysis, age and high SLC9A1 expression maintained an independent risk factor for OS among OC Table 1. Group with high-risk score tend to have higher levels of SLC9A1, EZR and HSPG2 expression and less survival compared with the low-risk group Figure 6B.

Results of GSEA

We further performed GSEA on the three key genes to discover signaling pathways that were distinguishingly activated in macropinocytosis. As shown in [Figure 6], different degrees of SLC9A1, EZR and HSPG2 expression were related to phagocytosis, focal adhesion, and endocytosis and glycolysis gluconeogenesis pathways in cancer. It showed that the three key hub genes may be closely related to macropinocytosis in OC.

The tissue-level of the key hub genes expression in HPA

SLC9A1, HSPG2 and EZR was mostly found in the cytoplasm or membranous of OC cells, as shown through searching their expressions in the HPA database Figure 6.

DISCUSSION

Macropinocytosis is a form of fluid-phase endocytosis in which cells use ruffles of the plasma membrane to take up medium into primary endocytic vesicles [13]. It is a nonspecific internalization process and has a vital role in the uptake of extracellular substances and antigen presentation. During tumor development, it helps cancer cells survive in nutrient-deficient environment to resistant to anticancer drugs, and promote invasion and metastasis [14]. This process depends on the activation of the RAS gene, growth factor receptors (GFRs), and other signal pathways [15,16].

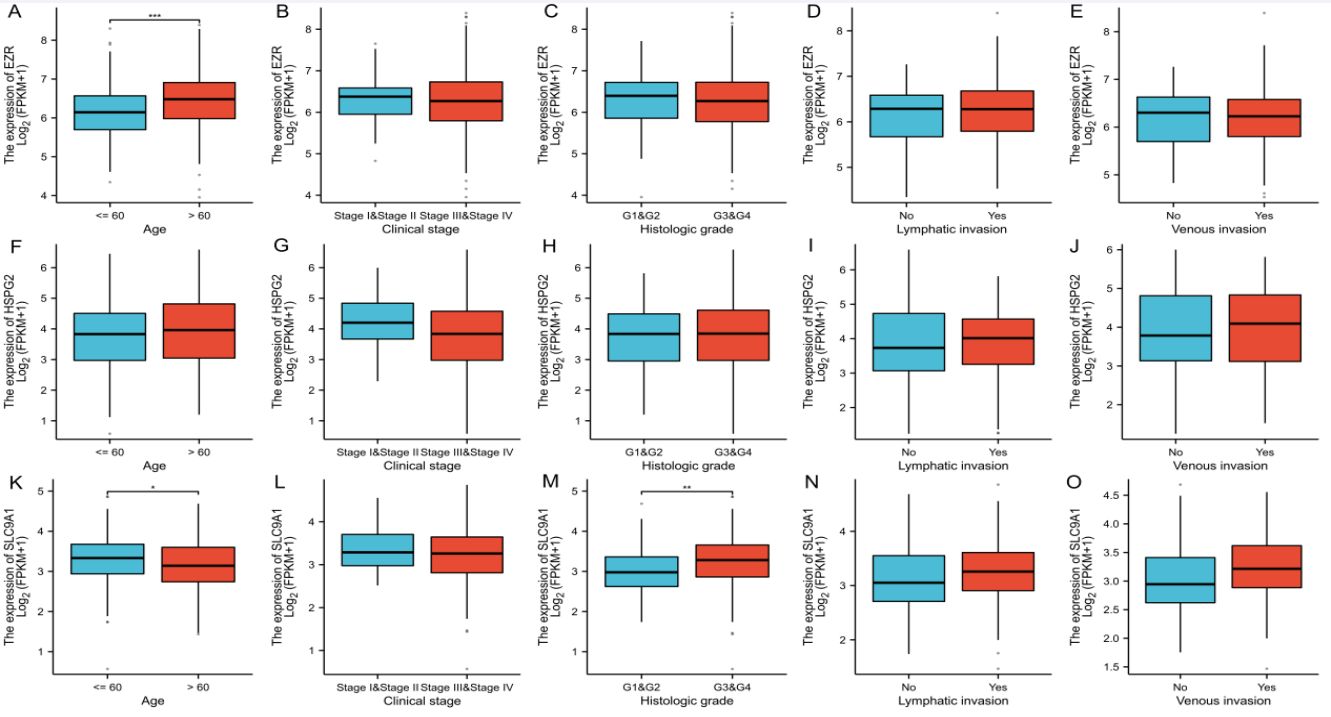

Figure 4 The correlation between the key hub genes (EZR, HSPG2 and SLC9A1) expression levels and various clinicopathological features in OC patients using Wilcoxon signed-rank test from the TCGA database. EZR (A) and SLC9A1 (K) expression level was significantly related to age (P<0.05). Higher SLC9A1 expression level was notably associated with high histologic grade (M, P<0.05). OC, ovarian cancer; EZR, Ezrin; HSPG2, Heparan Sulfate Proteoglycan 2; SLC9A2, Solute Carrier Family 9 Member A1; TCGA, the Cancer Genome Atlas.

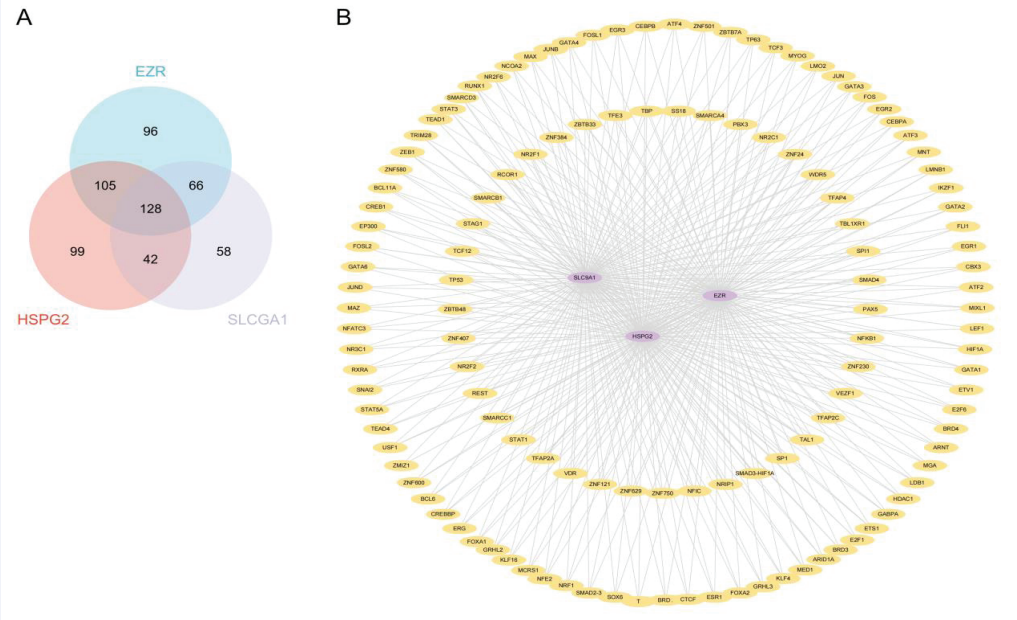

Figure 5 Identification of the common TFs of the key hub genes (EZR, HSPG2 and SLC9A1). (A). Intersection of all TFs of the key hub genes; (B). The common TFs related to the key hub genes were used to as nodes in an interconnected regulatory network. Light purple oval nodes represent the key hub genes, and TFs interact with genes as yellow oval nodes. TF, transcription factors; EZR, Ezrin; HSPG2, Heparan Sulfate Proteoglycan 2; SLC9A2, Solute Carrier Family 9 Member A1.

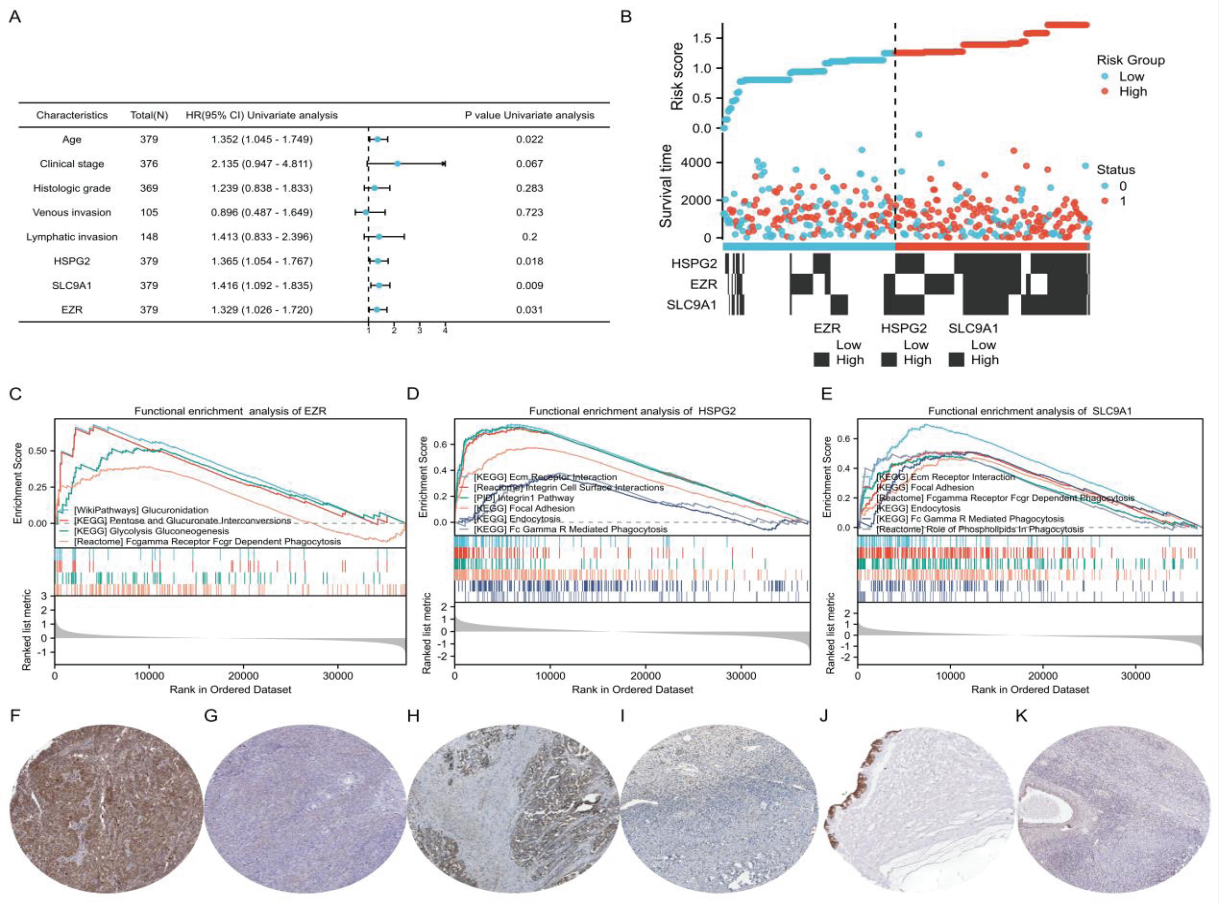

Figure 6 Construction of a risk prognostic model and enrichment plots in OC patients from GSEA based on the key hub genes (EZR, HSPG2 and SLC9A1). (A). Univariate Cox regression analysis was performed for the key hub genes. A value of P<0.05 was considerated statistically significant; (B) LASSO regression of the key hub genes; (C-E) Functional enrichment analysis of the key hub genes expression in OCs from TCGA, including EZR (C), HSPG2 (D) and SLC9A1 (E). (F-K). Expression of the key hub genes at the tissue level in the HPA database: (F-G) High level of EZR expression in OC tissue and negative expression in normal ovarian tissue; (H-I) Medium level of HSPG2 expression in OC tissue and negative expression in normal ovarian tissue; (J-K) High level of SLC9A1 expression in OC tissue and negative expression in normal ovarian tissue. OC, ovarian cancer; GSEA, Gene Set Enrichment Analysis; EZR, Ezrin; HSPG2, Heparan Sulfate Proteoglycan 2; SLC9A2, Solute Carrier Family 9 Member A1; TCGA, the Cancer Genome Atlas; HPA, Human Protein Atlas.

Epithelial-mesenchymal transition (EMT) is the key mechanisms that facilitate the cancer metastasis. It is often defined by the loss of the epithelial marker E-cadherin and the gain of the expression of the mesenchymal marker vimentin [17]. Extracelluar ATP (eATP) can be internalized into the lung cancer cells to trigger EMT via purinoceptor signals activated by P2X7. It can also activate production of matrix metallopeptidase (MMPs) and promote lung cancer cell shedding, EMT, migration, and invasion. During this process, Snail and Slug (and probably others), which is known as EMT TFs, was enhanced [5]. During the development of the neural crest cells migration, Cad6B is removed from premigratory neural crest cells through cell surface internalization events that include clathrin-mediated endocytosis and macropinocytosis. Both of these processes are dependent upon the function of dynamin, and inhibition of Cad6B internalization abrogates neural crests cell EMT and migration [6]. Accordingly, tumor cells utilize macropinocytosis to support energy, and may also internalize the adhesion receptor directly to reduce intercellular adhesion and promote migration capacity.

In the present study, we performed differential expression analyses of the ten candidate genes involved in macropinocytosis and prognostic of OC, then selected three key hub genes through PPI and a series of differential expression analyses and survival analyses between tumor and normal OC tissues. They were all overexpressed and significantly correlated with poor survival in OCs. Previous studies have found that EZR [18], HSPG2 [19] and SLC9A1 [20] were potential targets for the treatment of OC, which are consistent with our analysis results. Subsequently, patients with elevated SLC9A1 expression had an advanced histologic grade, however, the EZR and HSPG2 expression levels were not notably associated with the clinic pathological factors. We constructed a prognostic risk model using the three key hub genes through univariate Cox, multivariate Cox and Lasso

Cox regression analysis. Increased EZR, HSPG2 and SLC9A1 expression was related to poor OS by univariate Cox regression analysis. In multivariate Cox analysis, increased SLC9A1 expression maintained an independent risk factor for OS. Group with high-risk score tended to have higher levels of SLC9A1, EZR and HSPG2 expression and less survival compared with the low-risk group. Furthermore, the protein expression of the three key hub genes in OC patients and normal ovarian samples was testified by the HPA database.

Next, we conducted a framework to elucidate gene regulatory networks involving the common TFs from the three key hub genes. It has been reported that pancreatic ductal adenocarcinoma (PDAC) cells could escape autophagy inhibition via NRF2-induced macropinocytosis to upregulate and utilize nutrient [21]. In hepatocellular carcinoma cells, hypoxia-inducible factor (HIF)-1 activated the transcription of a membrane ruffling protein, EH domain-containing protein 2 (EHD2), to initiate macropinocytosis to harness extracellular protein as a nutrient to survive [22]. However, its function in OC remains to be addressed. These key hub genes may have the potential to be the promising biomarkers and new targets in therapeutic approaches for OC.

The functions of EZR, HSPG2 and SLC9A1 were investigated in OC from TCGA data by GSEA. Some signaling pathways such as Ecm Receptor Interaction, Integrin Cell Surface Interactions, Integrin1 Pathway, Focal Adhesion, Endocytosis, Fc Gamma R Mediated Phagocyosis, Fcgamma Receptor Fcgr Dependent Phagocytosis, as well as Glycolysis Gluconeogenesis that differentially enriched in high or low expression of the key hub genes were more comprehensively reported in the present study. These results suggested that EZR, HSPG2 and SLC9A1 may serve as prognostic markers and potential therapeutic targets in OC, which were not summarized in other bioinformatic analyses research of OC.

During the process of macropinocytosis formation, excessive activation of Ras or Rac GTPases can drive actin cytoskeleton remodelling causing plasma membrane ruffling and bulk engulfment of extracellular material [23]. Actin can drive protrusion at the plasma membrane, and plays a key role in sculpting membranes that drive endocytic uptake, trafficking, and recycling. Recycling of receptors such as integrins and receptor tyrosine kinases (RTKs) regulates adhesion to the ECM as well as actin organisation for migration towards nutrient gradients [24]. This mechanism is essential in recycling of proteins involved in invasion and metastasis including various integrins [25]. In non-small-cell lung cancer, upregulation of proteins involved in recycling such as clathrin light chain b (CLCb) and dynamin-1 (Dyn1) can enhance EGFR recycling to plasma membrane through clathrin-mediated endocytosis, leading to increased invasion and metastasis in vivo [26]. These processes depend on actin dynamics and are regulated by signals from membrane receptors and contact with the matrix. Accordingly, targeting macropinocytosis via the actin cytoskeleton or its regulators could be a potential therapeutic target.

During our analyses, EZR, HSPG2 and SLC9A1 was mainly enriched on integrin, adhesion and endocytosis pathway in OC, but the underlying relationship in the diagnosis and prognosis of OC remains unclear. Considering the combination of targeting macropinocytosis and OC metastasis, may provide new possibilities for OC diagnosis, prognosis, and treatment. They would be new potential targets of therapeutic drugs for OC.

CONCLUSIONS

Our research found the affinitive relationship between three macropinocytosis-related genes expression (EZR, HSPG2 and SLC9A1) and the prognosis of OC. Moreover, the Ecm Receptor Interaction, Integrin Cell Surface Interactions, Integrin1 Pathway, Focal Adhesion, Endocytosis, Fc Gamma R Mediated Phagocyosis, Fcgamma Receptor Fcgr Dependent Phagocytosis, and Glycolysis Gluconeogenesis may be the key pathways controlled by macropinocytosis-related genes in OC. Therefore, macropinocytosis-related genes may become important markers and new targets for early diagnosis, precise treatment, and prognostic assessment of OC.

FUNDING

This manuscript is supported by the grants as follows: Zhe jiang Provincial Traditional Chinese Medicine Science and Technology Project (2021ZB134); The seventh Batch of National Old Chinese Medicine Experts Academic Experience Inheritance Work Project (G.TCM.R.J.H.[2022]76); Zhe jiang Provincial Training program of young and middle-aged clinical famous TCM doctors (Zhejiang Medical Letter (2021) No. 9).

AUTHOR CONTRIBUTIONS

Formal analysis, data curation, wrings - original draft, validation and data analysis was performed by Ying shao. Visualization was performed by Shuai Huang. Yingshao and Zhaochun He conceived the idea, revised the manuscript and approved the final submission. All authors read and approved the final manuscript.

DATE AVAILABILITY

Any data and R script in this study can be obtained from the corresponding author upon reasonable request. In this study, TCGA and GTEx expression data set is available on the TCGA and GTEx data portal.

ACKNOWLEDGMENTS

We thank the TCGA and GTEx project teams for making the date available.

REFERENCES

1. Shao H, Im H, Castro CM, Breakefield X, Weissleder R, Lee H. New Technologies for Analysis of Extracellular Vesicles. Chem Rev. 2018; 118: 1917-1950.

2. Roy A, Zhao Y, Yang Y, Szeitz A, Klassen T, Li SD. Selective targeting and therapy of metastatic and multidrug resistant tumors using a

long circulating podophyllotoxin nanoparticle. Biomaterials. 2017; 137: 11-22.

3. Xiao F, Li J, Huang K, Li X, Xiong Y, Wu M, et al. Macropinocytosis: mechanism and targeted therapy in cancers. Am J Cancer Res. 2021; 11: 14-30.

4. Egami Y, Taguchi T, Maekawa M, Arai H, Araki N. Small GTPases and phosphoinositides in the regulatory mechanisms of macropinosome formation and maturation. Front Physiol. 2014; 5: 374.

5. Cao Y, Wang X, Li Y, Evers M, Zhang H, Chen X. Extracellular and macropinocytosis internalized ATP work together to induce epithelial-mesenchymal transition and other early metastatic activities in lung cancer. Cancer Cell Int. 2019; 19: 254.

6. Padmanabhan R, Taneyhill LA. Cadherin-6B undergoes macropinocytosis and clathrin-mediated endocytosis during cranial neural crest cell EMT. J Cell Sci. 2015; 128: 1773-1786.

7. Sun Z, Huang J, Su L, Li J, Qi F, Su H, et al. Arf6-mediated macropinocytosis-enhanced suicide gene therapy of C16TAB-condensed Tat/pDNA nanoparticles in ovarian cancer. Nanoscale. 2021; 13: 14538-14551.

8. Niu X, Gao Z, Qi S, Su L, Yang N, Luan X, et al. Macropinocytosis activated by oncogenic Dbl enables specific targeted delivery of Tat/pDNA nano-complexes into ovarian cancer cells. Int J Nanomedicine. 2018; 13: 4895-4911.

9. von Mering C, Huynen M, Jaeggi D, Schmidt S, Bork P, Snel B. STRING: a database of predicted functional associations between proteins. Nucleic Acids. Res 2003; 31: 258-261.

10. Chin CH, Chen SH, Wu HH, Ho CW, Ko MT, Lin CY. cytoHubba: identifying hub objects and sub-networks from complex interactome. BMC Syst Biol. 2014; 8: S11.

11. Lambert SA, Jolma A, Campitelli LF, Das PK, Yin Y, Albu M, et al. The Human Transcription Factors. Cell. 2018; 172: 650-665.

12. Zhou KR, Liu S, Sun WJ, Zheng LL, Zhou H, Yang JH, et al. ChIPBase v2.0: decoding transcriptional regulatory networks of non-coding RNAs and protein-coding genes from ChIP-seq data. Nucleic Acids Res. 2017; 45: D43-D50.

13. Kay RR. Macropinocytosis: Biology and mechanisms. Cells Dev. 2021; 168: 203713.

14. Qiu Z, Liu W, Zhu Q, Ke K, Zhu Q, Jin W, et al. The Role and Therapeutic Potential of Macropinocytosis in Cancer. Front Pharmacol. 2022; 13: 919819.

15. Hesketh GG, Papazotos F, Pawling J, Rajendran D, Knight JDR, Martinez S, et al. The GATOR-Rag GTPase pathway inhibits mTORC1 activation by lysosome-derived amino acids. Science. 2020; 370: 351-356.

16. Hobbs GA, Baker NM, Miermont AM, Thurman RD, Pierobon M, Tran TH JM, et al. Atypical KRAS(G12R) Mutant Is Impaired in PI3K Signaling and Macropinocytosis in Pancreatic Cancer. Cancer Discov. 2020; 10: 104-123.

17. Pastushenko I, Blanpain C. EMT Transition States during Tumor Progression and Metastasis. Trends Cell Biol. 2019; 29: 212-226.

18. Gov E. Co-expressed functional module-related genes in ovarian cancer stem cells represent novel prognostic biomarkers in ovarian cancer. Syst Biol Reprod Med. 2020; 66: 255-266.

19. Bieńkowska A, Ducher M, Orzechowska M, Słyk Ż, Ciepiela O, Jaworowski J, et al. Increased temperature-related adeno-associated virus vectors transduction of ovarian cancer cells - essential signatures of AAV receptor and heat shock proteins. Exp Ther Med. 2019; 18: 4718-4732.

20. Sanhueza C, Araos J, Naranjo L, Toledo F, Beltrán AR, Ramírez MA, et al. Sodium/proton exchanger isoform 1 regulates intracellular pH and cell proliferation in human ovarian cancer. Biochim Biophys Acta Mol Basis Dis. 2017; 1863: 81-91.

21. Su H, Yang F, Fu R, Li X, French R, Mose E, et al. Cancer cells escape autophagy inhibition via NRF2-induced macropinocytosis. Cancer Cell. 2021; 39: 678-693.e611.

22. Zhang MS, Cui JD, Lee D, Yuen VW, Chiu DK, Goh CC, et al. Hypoxia-induced macropinocytosis represents a metabolic route for liver cancer. Nat Commun. 2022; 13: 954.

23. Kerr MC, Teasdale RD. Defining macropinocytosis. Traffic. 2009; 10: 364-371.

24. Steinberg F, Gallon M, Winfield M, Thomas EC, Bell AJ, Heesom KJ, et al. A global analysis of SNX27-retromer assembly and cargo specificity reveals a function in glucose and metal ion transport. Nat Cell Biol. 2013; 15: 461-471.

25. Caswell PT, Chan M, Lindsay AJ, McCaffrey MW, Boettiger D, Norman JC. Rab-coupling protein coordinates recycling of alpha5beta1 integrin and EGFR1 to promote cell migration in 3D microenvironments. J Cell Biol. 2008; 183: 143-155.

26. Chen PH, Bendris N, Hsiao YJ, Reis CR, Mettlen M, Chen HY, et al. Crosstalk between CLCb/Dyn1-Mediated Adaptive Clathrin-Mediated Endocytosis and Epidermal Growth Factor Receptor Signaling Increases Metastasis. Dev Cell. 2017; 40: 278-288.e5.